energies

MDPI

Article

Geothermal Power Production from Abandoned Oil Reservoirs Using In Situ Combustion Technology

Yuhao Zhu [1], Kewen Li [1,2,3,*], Changwei Liu [4,*] and Mahlalela Bhekumuzi Mgijimi [1]

1 School of Energy Resources, China University of Geosciences, Beijing 100083, China; yuhao_zhu@cugb.edu.cn (Y.Z.); mahlalelab@cugb.edu.cn (M.B.M.)
2 Key Laboratory of Strategy Evaluation for Shale Gas, Ministry of Land and Resources, Beijing 100083, China
3 Department of Energy Resources Engineering, Stanford University, Stanford, CA 94305, USA
4 School of Earth Sciences and Resources, China University of Geosciences, Beijing 100083, China
* Correspondence: likewen@cugb.edu.cn (K.L.); cwliu@cugb.edu.cn (C.L.)

Received: 11 October 2019; Accepted: 20 November 2019; Published: 24 November 2019

Abstract: Development of geothermal resources on abandoned oil reservoirs is considered environmentally friendly. This method could reduce the rate of energy consumption from oil fields. In this study, the feasibility of geothermal energy recovery based on a deep borehole heat exchanger modified from abandoned oil reservoirs using in situ combustion technology is investigated. This system could produce a large amount of heat compensated by in situ combustion in oil reservoir without directly contacting the formation fluid and affecting the oil production. A coupling strategy between the heat exchange system and the oil reservoir was developed to help avoid the high computational cost while ensuring computational accuracy. Several computational scenarios were performed, and results were obtained and analyzed. The computational results showed that an optimal water injection velocity of 0.06 m/s provides a highest outlet temperature of (165.8 °C) and the greatest power output of (164.6 kW) for a single well in all the performed scenarios. Based on the findings of this study, a geothermal energy production system associated with in situ combustion is proposed, specifically for economic reasons, because it can rapidly shorten the payback period of the upfront costs. Modeling was also performed, and based on the modeling data, the proposed technology has a very short payback period of about 4.5 years and a final cumulative net cash flow of about $4.94 million. In conclusion, the present study demonstrates that utilizing geothermal resources or thermal energy in oilfields by adopting in situ combustion technology for enhanced oil recovery is of great significance and has great economic benefits.

Keywords: geothermal power production; abandoned oil reservoirs; in situ combustion

1. Introduction

Generating geothermal power from abandoned oil reservoirs could be the answer to the energy crisis facing today's world. However, the upfront cost in a geothermal project is a barrier. Increasing the heat production and shortening the payback period of the upfront costs are two main objectives in a geothermal project. High outlet temperature and larger amount of geothermal fluid extraction could help to enhance the total heat production, whereas low drilling costs are conducive to reduce the payback period of the geothermal project. In this regard, most oilfields possess great potential for producing geothermal energy, because they are associated with production of geothermal fluid from oil reservoirs. Furthermore, abandoned oil reservoirs are good potential areas for harvesting and producing geothermal energy, and are most favorable because they are easily retrofitted into geothermal wells. However, the outlet temperature of geothermal wells in oil fields is usually lower, thus resulting in low heat production and long payback period.

Over recent years, the petroleum industry has seen and experienced rapid development due to the high demand of energy worldwide. In the midst of this rapid development, a larger number of oil and gas wells has been left abandoned due to either technical problems or economic benefit limitations, particularly heavy oil reservoirs. To enhance heavy oil recovery, thermal recovery technology such as in situ combustion method is often used. According to the latest update on drilled oil wells data, there exist about 20–30 million abandoned oil wells around the world [1]. Abandoned oil reservoirs may not hold oil productivity after a long-term recovery process, but such wells can produce brine fluids with high temperature. Thus, geothermal energy from such high-temperature fluids could be directly or indirectly recovered back to the surface for further utilization. Li et al. [2] and Zhang et al. [3] proposed a geothermal system combined with power generation which extracts geothermal heat from hot water in oilfields. Zheng et al. [4] proposed a concept to produce geothermal energy from abandoned oil and gas reservoirs by oxidizing the residual oil with injected air. This system, however, lacks a detailed heat exchanger model describing the heat transfer from reservoir to geothermal well, which is the essential part of evaluating the efficiency of a geothermal system. Zheng et al. [4] proposed a concept which lacks a detailed heat exchanger model, Davis and Michaelides [5] investigated the feasibility of the heat exchanger using abandoned wells for power generation by ORC (Organic Rankine Cycle). Their proposed geothermal system can provide an output power of 3.4 MW when at optimal condition.

Wight and Bennett [6] pointed out that the closed loop system (i.e., heat exchanger) retrofitted from abandoned oil well has the advantage of protecting both the equipment and the environment from performance or safety risks caused by minerals and contaminants commonly present in naturally occurring geothermal fluid. This is because the system can produce geothermal energy without extracting geothermal fluid from the formation. Another advantage of utilizing abandoned oil reservoirs is that there is little or no drilling cost at all, which is generally the main upfront investment in any geothermal project [7]. Moreover, the cost of retrofitting abandoned oil well into geothermal well using work-over techniques is equivalent to one tenth the cost of drilling a new geothermal well, and the maximum expense is even less than one seventh of the cost of drilling a new well [8]. Therefore, with regard to the above, it is clear that, if abandoned wells could be re-developed and utilized, large amount of drilling cost could be cut down, and more economic gains could be achieved.

Numerous mathematical models have been developed to both calculate the outlet temperature and evaluate the performance of the heat exchanger. Bu et al. [8] considered a two-dimensional model for numerically simulating the heat transfer between the surrounding rocks and the heat exchanger. This model neglects the variation of temperature in the tube wall of the injection annulus and the extraction well, which decreases the accuracy of the temperature distribution and overestimates the heat extracted from the surrounding rocks. Furthermore, Nian and Cheng [9] pointed out that it is unsound to use the assumption of vanishing well radius as a boundary condition in the model, because this could overestimate the heat flux from the surrounding rocks to working fluid in the heat exchanger.

Noorollahiet et al. [10] simulated a geothermal system which extracted geothermal energy by using two abandoned oil wells in Ahwaz oil field in Southern Iran. They developed a 3D numerical model using finite element method software ANSYS. They found that the sensitive parameter analysis indicates that casing geometry will strongly affect the heat transfer between the geothermal well and the surrounding rocks. Mokhtari et al. [11] found that when evaluating the pressure drop and thermal efficiency of the heat exchanger, the diameter ratio of the inner to outer pipe is very important. Their results showed that the optimal diameter ratios for pressure drop minimization and thermal efficiency maximization are 0.675 and 0.353, respectively.

In general, there are three grades of temperatures for extractive geothermal energy recognized by the industry namely: high temperature (>180 °C), intermediate temperature (100 to 180 °C) and low temperature (30 to 100 °C), respectively [12]. High-temperature geothermal resources can be used for power generation, while the low and medium temperature resources could be/are normally used directly for district heating and geothermal source heat pump (GSHP) [13,14]. However, a large number of geothermal reservoirs have low outlet temperatures. Low-temperature geothermal resources are

economically not viable for commercial plants because they cannot generate sufficient heat. Thus, they cannot recover the upfront investment for retrofitting the abandoned wells and the construction of the power plants. To extract more heat from subsurface reservoir, low boiling point organic fluids with high heat-to-electricity efficiency are often used as working fluid mostly in ORC plants. Mokhtari et al. [11] investigated four organic fluids (R123, R134a, R245fa, R22) often used as working fluids in geothermal power plants. They found that R123 has the most desirable characteristics in comparison with other working fluids. Noorollahi et al. [15] further investigated two other types of working fluid (isobutene and ammonia) for power generation. A binary power cycle model was applied for power generation in their study to calculate the total electric power output. The two fluids (ammonia and isobutene) were chosen as secondary fluids in their power cycle, and their power outputs were compared. They found that for similar flow rates, the total net power for isobutene is greater than that of ammonia.

Another method for enhancing geothermal system is extracting geothermal energy from oil reservoirs with in situ combustion. Zheng et al. [4] proposed a geothermal system enhanced by oil reservoir using in situ combustion technology. They used a retrofitted abandoned well for their geothermal system. Similarly, Cinar [16] proposed a geothermal model using a perforated well to extract heated fluid from the oil reservoir where wet in situ combustion was applied. However, as pointed out in his study, wet in situ combustion may extinguish the combustion process, which causes reduction in the mass production of heated water resulting into less sufficient heated water to sustain a commercial scale power plant. Additionally, this may also result in the large depletion of the formation fluid. Cheng et al. [17] investigated the enhancement effect of geothermal power generation from abandoned oil reservoirs with thermal reservoirs. They found that a geothermal well with thermal reservoirs could produce a heat and electric power output of about four times the amount that can be produced by a geothermal well without thermal reservoirs. Although the cost of drilling can be reduced or even eliminated, the cost of the power plant installation accounts for the major portion of the total investment of the geothermal project, which further prolongs the payback period. Therefore, in this regard, more heat extraction from the subsurface is needed to sustain a commercial-sized geothermal project/plant.

In this study, a new model for recovering and re-utilizing oil for geothermal energy from abandoned wells is proposed. For this model, an in situ combustion technique is applied in the reservoir to recover heavy oil by injecting air into the formations. The air injection helps to oxidize the oil and heat up the reservoir. A schematic representation of the newly proposed model can be seen in Figure 1.

Figure 1 is a schematic representative summary of the development and utilization of the resources in abandoned oil reservoirs by in situ combustion. As can be seen from the figure, during the recovery process, a large amount of heat is generated from the in situ combustion. The abandoned well becomes a heat exchanger (i.e., geothermal well). A schematic representation of the heat exchange system is shown in Figure 2.

As can be seen from Figure 2, water is injected through the injection annulus and extracted through the extraction well. The oil reservoir with in situ combustion provides large amounts of heat at the bottom of the geothermal system. The system mainly includes heat transfer in the geothermal well (i.e., extraction well and injection annulus), oil reservoir and the surrounding rocks (i.e., strata). In general, the geothermal fluid extraction process may cause some problems in the formation, including groundwater recession, corrosion and scaling problem, the high cost of geothermal, and drilling of the re-injection well [18]. However, the system shown in Figure 2 has no direct contact in the formation fluid and no effect on oil production. It only extracts the heat from the formation and the oil reservoir by recycling the working fluid in a closed loop concentric tube, which is combined with in situ combustion by air injection in the oil reservoir. The detailed methodology adopted in this study is shown in Figure 3.

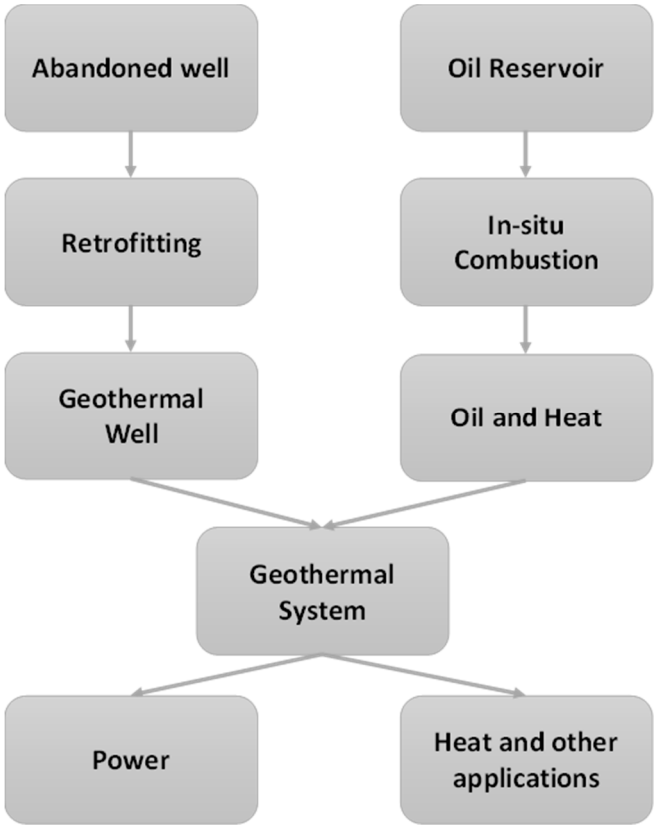

Figure 1. A new method of geothermal production utilizing abandoned wells and in situ combustion.

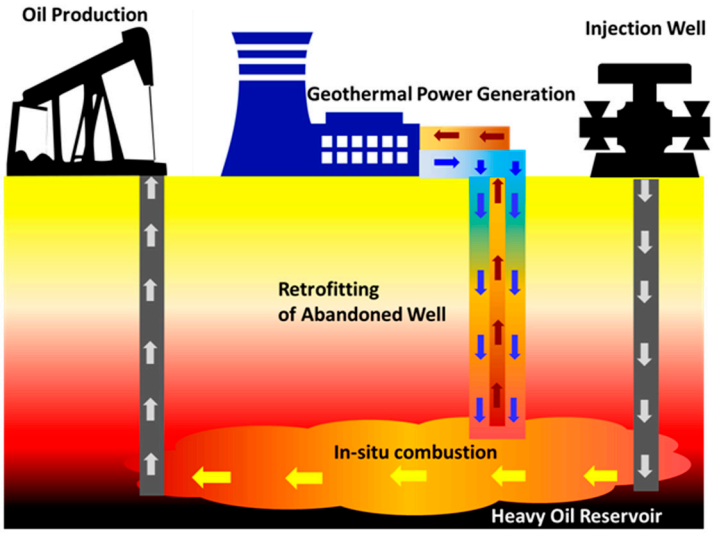

Figure 2. Schematic of heat exchange system.

In this study, a numerical model describing retrofitting abandoned oil wells into useful geothermal wells with in situ combustion for the purpose of recovering geothermal resources was developed. This model provides a new coupling strategy between the heat exchange system and the oil reservoir. The main idea is that the reservoir temperature with in situ combustion is expressed as a function of time, and then imported into the heat exchange system as a boundary condition. This model takes advantage of the commercial reservoir simulator CMG for simulating in situ combustion and helps to avoid large amounts of computational cost when calculating the heat transfer from the surrounding rocks and oil reservoir to the heat exchanger. Several parameters known to affect the system performance

were analyzed using the proposed model in this study. Moreover, it should be noted that turbulent flow, which increases the computational efficiency without losing much computational accuracy is not considered in this model. For the findings of this study, the computational results indicate that the outlet temperature increases remarkably after the combustion front reaches the area near the heat exchange wellbore. Furthermore, a geothermal system using advanced in situ combustion was proposed to extract more heat from the reservoir right from the beginning, thereby significantly shortening the payback period of the upfront costs.

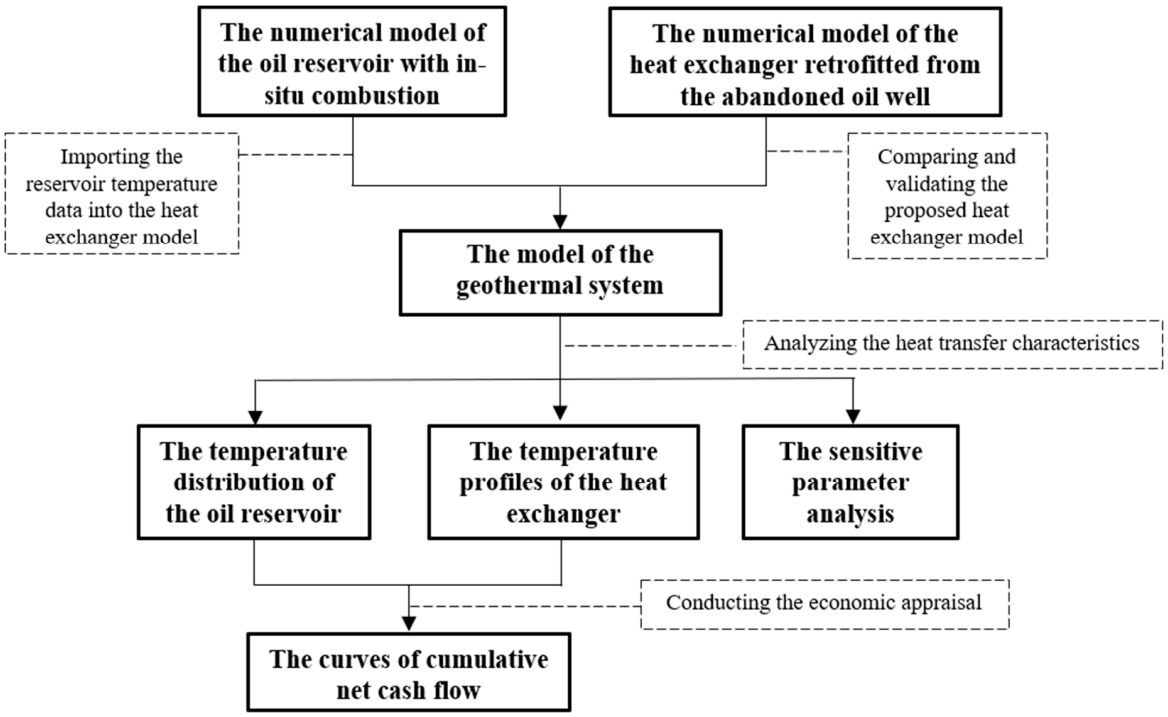

Figure 3. Flowchart followed when investigating the proposed geothermal system.

2. Model Description of In Situ Combustion

The process of in situ combustion is basically the injection of oxidized gas or oxygen-enriched air to generate heat by burning a portion of residual oil, where most of the oil is driven toward the producers by a combination of gas-drive, steam or water-drive. The main purpose of applying in situ combustion is to generate a large amount of heat for the geothermal system. For this study, the modeling was performed using STARS by CMG. The in situ combustion model assumes that the reservoir has: uniform porosity, isotropic permeability, and closed upper and lower layers. The model utilizes a five spots pattern, as shown in Figure 4.

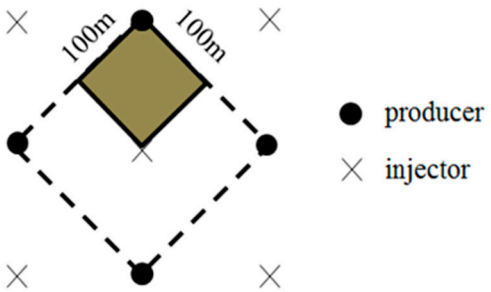

Figure 4. Five spots pattern applied in oil reservoir model.

The numerical model domain, which is the dark area shown in Figure 4, takes advantage of the symmetric flow, with injection in one quarter and a production well in two corners. To simulate the process of in situ combustion in a general form, a direct conversion cracking kinetics scheme for three components of oil was chosen in the simulation, as it does not depend upon the stoichiometry of the products, and thus reduces the degree of uncertainty in the simulation results, as the number of unknowns is reduced [19]. Here we applied the chemical reaction data of the template in STARS of CMG [20] to obtain a typical in situ combustion scenario. Seven components were considered in the process of in situ combustion, and these were: water (H_2O), heavy oil component (HC), light oil component (LC), inert gas (IG), oxygen (O_2), carbon dioxide (CO_2), and coke, respectively. Three chemical reactions were introduced to describe the components change in reservoirs and the heat generated in the process. The enthalpy and activation energy of these three reactions were as shown in Table 1.

Table 1. Combustion reactions and their respective kinetic parameters.

Combustion Reaction	Activation Energy (J/gmole)	Enthalpy (J/gmole)
HC→10LC + 20coke	2.463 × 105	−6.86 × 106
HC + 16O_2→12.5H_2O + 5LC + 9.5CO_2 + 1.277IG + 15coke	8.41 × 104	6.29 × 106
Coke + 1.225O_2→0.5H_2O + 0.95CO_2 + 0.2068IG	5.478 × 104	5.58 × 105

Their relative permeability curves and the reservoir properties are shown in Table 2 and Figure 5.

Table 2. STARS input parameters for in situ combustion model.

Parameters	Values
Dimension	100 m × 100 m × 10 m
Grid (i, j and k)	20 × 20 × 5
Permeability	10 mD in i and j direction, 5 mD in k direction
Porosity	0.27
Thermal conductivity of reservoir rock	6 × 10^5 J/(m·day·K)
Overburden and under-burden volumetric heat capacity	2.350 × 10^6 J/(m^3·K)
Overburden and under-burden thermal conductivity	1.496 × 10^5 J/(m·day·K)
Oil saturation	0.4
Initial temperature	135 °C at 4 km, geothermal gradient 3 °C/km
Initial pressure	40 MPa at 4 km, pressure gradient 10 MPa/km
Well pattern	1/4 injectorlocatedat0, 0mand 1/4 producer located at 100, 100 m; both wells fully penetrate the reservoir
Air injection and oil production	5000 m^3/day and 5 m^3/day for both 1/4 wells

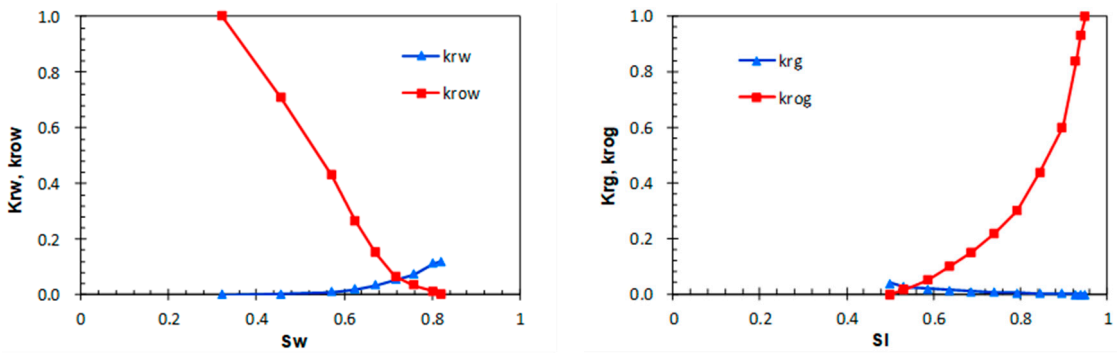

(**a**) Water–oil (**b**) Liquid–gas

Figure 5. Relative permeability curves used in model simulation.

3. Model Description of Geothermal Well

As seen in Figure 2, an abandoned well can be retrofitted into geothermal well by coating the inner tubing (extraction well) with insulation and sealing the bottom of the well. Water is then used as working fluid, and is injected through the annulus space and extracted from the inner tubing to the surface [21]. When the water flows downward along the annulus, it is heated by the surrounding rocks and by the reservoir, where there is a large amount of heat generated by in situ combustion. The heated water is then extracted back to the surface. This is a concentric tube heat exchanger, and the working fluid is not in direct contact with the surrounding rocks. Based on the data of the main oil fields in China, the geothermal gradient is generally about 0.03 K/m [22–26]. The model developed in this study utilized a concentric tube heat exchanger that was designed to retrofit an abandoned well with a typical casing outer diameter of 19.6 cm and an inner diameter of 15 cm. The inner diameter of the extraction well was 4 cm, the thickness of insulation was 2 cm, the well depth was 4000 m, and the thickness of the reservoir was 10 m. The whole reservoir was fully penetrated by the well. This system was modeled with the finite element modeling software COMSOL Multiphysics.

3.1. Governing Equations

A two-dimensional axi-symmetric cylindrical model was applied to describe the whole system. Heat exchange takes place between the working fluid and the rocks simultaneously [21,27], see Figure 6.

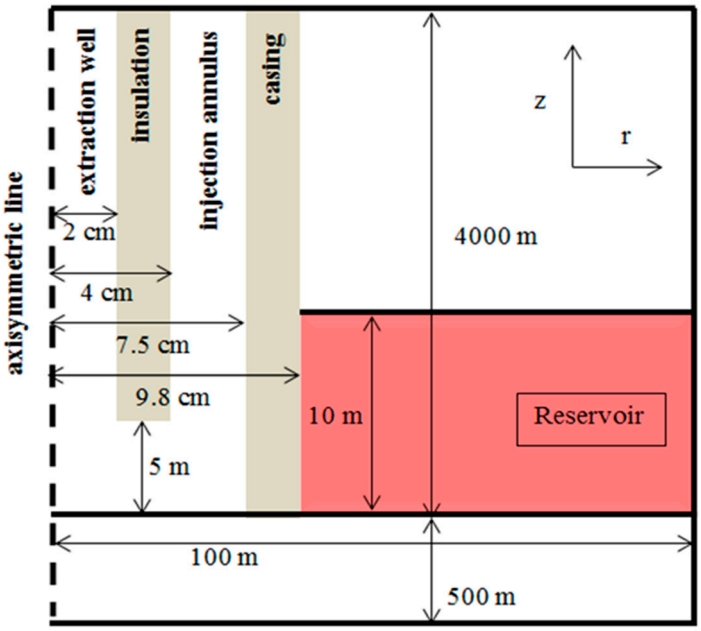

Figure 6. Dimensions of concentric pipe heat exchange system.

The dashed vertical line on the left side of Figure 6 shows the axis of symmetry, which is parallel to the direction of the z axis. The total depth of the heat exchange system is 4000 m from the surface. There is a buffer zone of 5 m at the bottom of the heat exchange system. The thickness of the oil reservoir is 10 m. The time-dependent governing equation corresponds to the convection-diffusion equation, which contains additional contributions of heat flux and no other heat source [28]. The heat flux describes the heat transfer from the rock to the injection annulus and from the injection annulus to the extraction well. Therefore, the expressional equation is

$$\rho C_p \frac{\partial T}{\partial t} + \rho C_p \vec{u} \cdot \nabla T + \nabla \vec{q} = 0 \quad (1)$$

where ρ is the density (kg/m^3), C_p is the specific heat capacity (J/(kg·K)), T is the absolute temperature (K), $\vec{u}$ is the velocity vector (m/s) and $\vec{q}$ is the heat flux by conduction (W/m^2), which can be described using the Fourier's three-dimensional diffusion law

$$\vec{q} = -k\nabla T \tag{2}$$

where k is thermal conductivity (W/(m·K)). Some parameters used in the numerical simulation are listed in Table 3. This heat transfer equation is already built into COMSOL, and can be called up in the software directly.

Table 3. The parameters used in the numerical simulation of the concentric tube heat exchanger.

Properties	Heat Capacity (J/kg·K)	Thermal Conductivity (W/(m·K))	Density (kg/m^3)
Casing	450	60	7850
Insulation	1010	0.025	1.225
Rock	1000	2	2200

For the water, the values of heat capacity, density and thermal conductivity depend on temperature and are already built into the COMSOL materials database, being expressed by the following formulas:

$$C_{p\_water} = 12010.1 - 80.4 \times T + 0.3 \times T^2 - 5.4 \times 10^{-4} \times T^3 + 3.6 \times 10^{-7} \times T^{-4} \tag{3}$$

$$\rho_{\_water} = 838.5 + 1.4 \times T - 0.003 \times T^2 + 3.7 \times 10^{-7} \times T^3 \tag{4}$$

$$k_{\_water} = -0.9 + 0.009 \times T - 1.610^{-5} \times T^2 + 8.010^{-9} \times T^3 \tag{5}$$

3.2. Initial Conditions

The velocity and the initial temperature of the injected water are both uniform along the well, and their values are 0.03 m/s and 30 °C, respectively. It should be noted that the velocity of water in the extraction well should be a corresponding value in order to retain a constant mass flow rate in the numerical model. The surface temperature is 15 °C. The initial temperature of the rocks is given by the following equation

$$T_{R,0}(z) = T_{srf} + G{\cdot}z \tag{6}$$

where $T_{R,0}$ is the initial rock temperature (K), T_{srf} is the temperature at surface (K), G is the geothermal gradient (K/m), and z is the depth of rock (m).

3.3. Boundary Conditions

The radius of influence may be at a modest distance from the well over the time frame modeled in this study. Therefore, the approximation that the temperature is constant at a 100-m radius is justified. The chosen distance of 100 m is explained in the following section. The boundary condition of the whole system, including the rock, is given by

$$T_{R,b}\Big|_{\substack{r=R \\ z=Z}} = T_{R,0}(z) \tag{7}$$

where $T_{R,b}$ is the rock temperature at a constant temperature boundary (K), R and Z are distances at constant temperature boundary in r and z direction (m).

However, if in situ combustion is applied in the reservoir, the boundary condition at the depth of the reservoir corresponds to the temperature influenced by the in situ combustion. Hence, the boundary condition at the depth of reservoir is given by

$$T_{R,b}\big|_{r=R} = T_{ic}(z,t) \tag{8}$$

where T_{ic} is the temperature of reservoir with in situ combustion and it is the function of depth z and time t. Please note that the distance of the constant temperature boundary is still R. This is reasonable, given that the influence of the in situ combustion on the heat exchange system is dominant considering the whole region of the oil field, while the reduction of the reservoir temperature and the heat extraction caused by geothermal well is limited.

4. Results and Discussion

A two-dimensional axi-symmetric cylindrical geothermic model was applied to simulate the temperature distribution of the geothermal well system as well as the surrounding rock system. To obtain more accurate temperature data, the two systems were coupled by using COMSOL Multiphysics simulator.

4.1. Mesh Independence Study

Before applying the heat exchanger model to calculate the outlet temperature, a mesh independence study was conducted to obtain stable temperature data. Triangular meshing was applied to the numerical model of the heat exchanger. The outlet temperatures after 5 years of operation are shown in Figure 7. When the number of triangular elements is small, the outlet temperature data oscillate and then begin to converge at certain values as the number of triangular elements becomes larger than 60,000. The numerical model of the heat exchanger in this study had 64,426 triangular elements, which guaranteed the mesh independence while using a relatively small computational time.

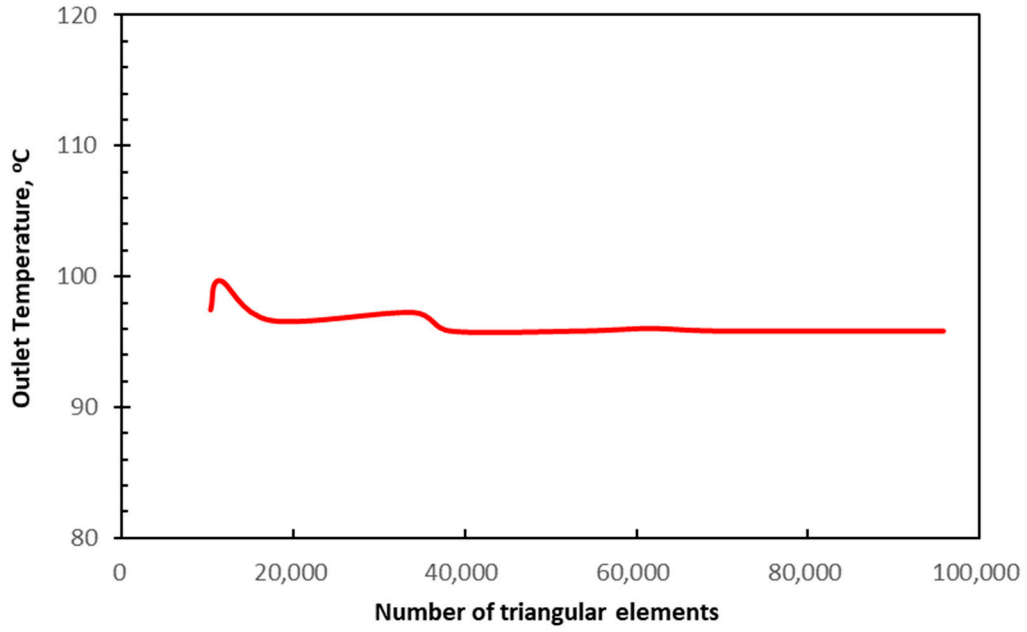

Figure 7. The outlet temperature at different numbers of triangular elements in the numerical model.

4.2. Validation and Comparison of the Model

The proposed model was compared and validated with the results from Bu et al. [8] and Templeton et al. [29]. The assumptions made by Bu et al. [8] include neglecting the variation of the tube

wall temperature of the injection annulus and the extraction well, and also the Dittus-Boelter relation in the convection model. These assumptions decrease the accuracy of the temperature distribution and will overestimate the heat extracted from the surrounding rocks in their system. Furthermore, the temperature transfer is very sensitive to the properties of the extraction well and the insulation. Again, the Dittus-Boelter relation is not suitable for parts with larger temperature differences, especially near the top of well, and is also not suitable for the annular injection well [30]. For the model used by Templeton et al. [29], the whole simulation domain does not consider the rock below the heat exchanger. It should be noted that both studies neglect the changes in the thermal properties of water, which are a function of temperature.

To achieve fair comparison with the newly proposed model in this study, we applied parameters similar to those applied in the two studies done by Bu et al. [8] and Templeton et al. [29]. To be more precise, the inner diameter of the extraction and the injection wells are 10 cm and 30 cm; the thickness of the insulation is 1 cm; the thickness of casing is 2 cm; the thermal conductivity of the surrounding rocks and the insulation are 2.1 W/(m·K) and 0.027 W/(m·K); the density and the heat capacity of the surrounding rocks are 2730 kg/m^3 and 1098 J/kg/K; and the velocity of the injected water and the geothermal gradient are 0.03 m/s and 0.045 K/m, respectively. Figure 8 shows the outlet temperatures calculated by these three models over ten years.

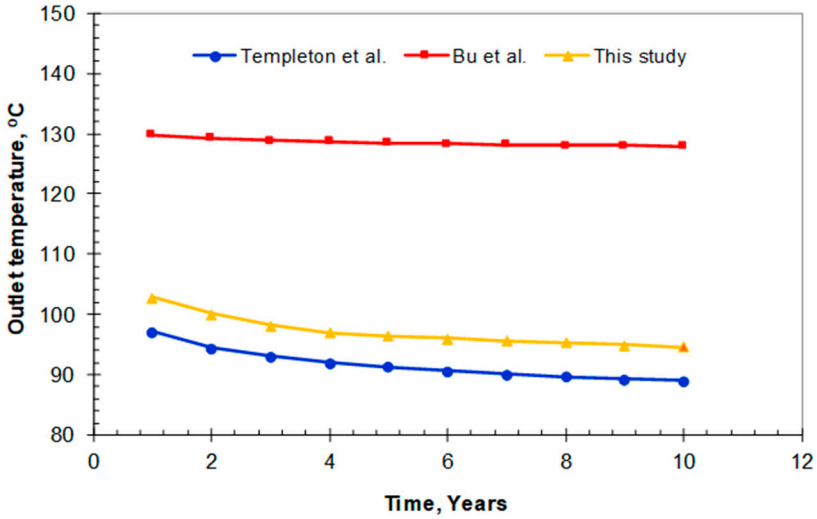

Figure 8. Verification and comparison of the results calculated by Bu et al. and Templeton et al. with the results of the proposed model under similar conditions.

As seen from Figure 8, the temperature result calculated by Bu et al. [8] model is about 26% to 44% higher than the results of both the model of Templeton et al. [29] and the proposed model in this study under similar conditions. The overestimation of the model proposed by Bu et al. [8] is because of the assumptions applied in the model, as mentioned in the previous section. The results of both the model of Templeton et al. [29] and the proposed model in this study have a similar shape of trend throughout the operational time/period. However, the negligence of the surrounding rocks below the heat exchange system causes the temperature result of the model of Templeton et al. [29] to be slightly smaller than the result of the proposed model in this study. Figure 9 shows the temperature profile of the injection annulus and the extraction well with 0.03 m/s injection velocity after a period of two months in operation.

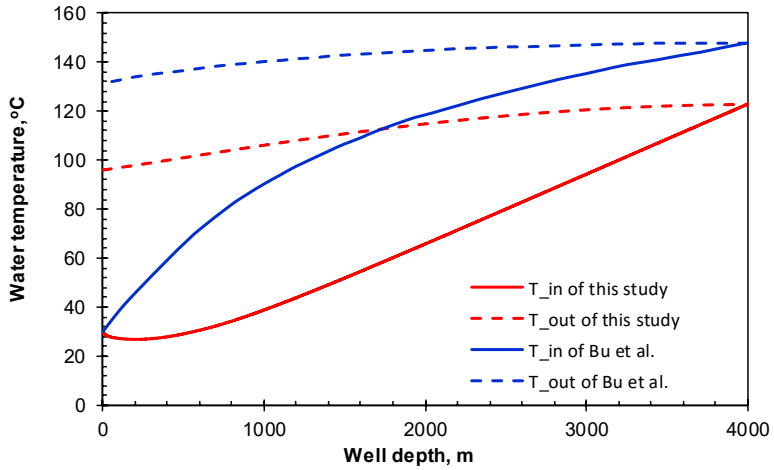

Figure 9. Comparison of the temperature profile between the proposed model of this study and the model of Bu et al.

As seen from Figure 9, the solid lines and the dashed lines show the temperature profiles of the injection annulus and extraction well, respectively. The highest temperature is found at the bottom of the well at about 4000 m. The variation of the fluid temperature curves of this study (red line) show that there is a slight decrease in the temperature near the top of the injection annulus. The reason for this is that the temperature of the injected water is 30 °C, and this is higher than that of the surface temperature, which is 15 °C. This causes the injected water to lose some heat in some regions near the wellhead. However, we cannot find any such phenomenon in the results from the model of Bu et al. [8]; thus, this overestimation reduces the accuracy of the simulation results of the model of Bu et al. [8].

4.3. Analysis of Heat Transfer Characteristics

The parameters applied in the calculation are listed in Tables 2 and 3, and Figures 5 and 6. The temperature distribution in the surrounding rocks and the heat exchange system with in situ combustion are shown in Figure 10.

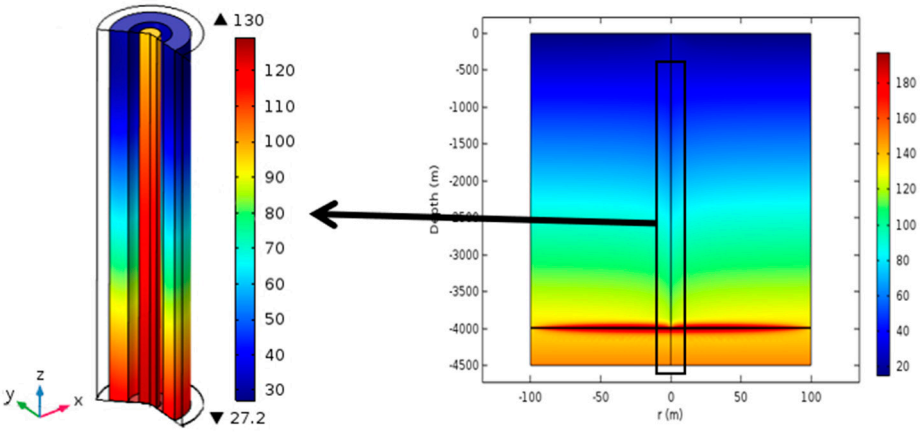

Figure 10. The temperature distribution of the heat exchange system after one year of operation (left figure), and the temperature distribution of the surrounding rocks after 50 years of operation (right figure).

As seen in Figure 10, there is a temperature drawdown near the heat exchange system. The high temperature zone is strongly marked at the depth of the in situ combustion reservoir at about 4000 m. The isothermal contours show that the initial geothermal temperature is not affected by the heat exchange system when the radius is greater than 80 m, even after a period of 50 years of operation.

This could help to explain why the 100 m distance (the radius of influence in boundary conditions) from the heat exchange system to the rock in the *r*-direction, and the 500 m distance in the *z*-direction, were chosen as the boundary of the surrounding rocks for the model proposed in this study.

4.4. Heat Production Analysis

Considering the high upfront investment required for the initial development of the geothermal power plant and retrofitting of the abandoned well, the outlet temperatures of the conventional geothermal well project may not be high enough to generate enough electric energy and recover the upfront costs. Therefore, in order to obtain more heat from the reservoir, in situ combustion was applied to supply the heat extraction from the heat exchange system. A three-dimensional model of the reservoir with in situ combustion was simulated by using the STARS simulator in CMG. The modeling grid numbers are: 20, 20 and 5 in the i, j and k directions, respectively. The temperature distributions in the oil reservoir during the 6th year and 11th year of the total operation period of 50 years are shown in Figure 11. The measurement unit of the temperatures of the reservoir is degrees Celsius.

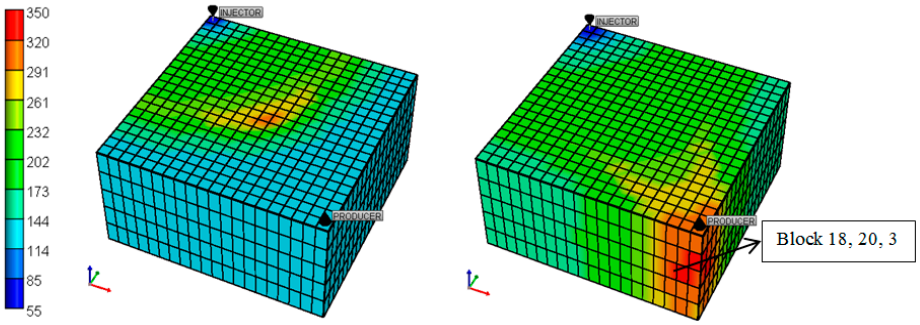

Figure 11. The temperature distribution of the oil reservoir at the 6th year (left figure) and the 11th year (right figure).

In Figure 11, the air is injected from the upper left injector. The lower right producer will be retrofitted into the heat exchange system. The extreme high temperature zone in this figure is where the combustion front is located. The temperature near the wellbore (block 18, 20, 3) and the average temperature of the whole reservoir are shown in Figure 12.

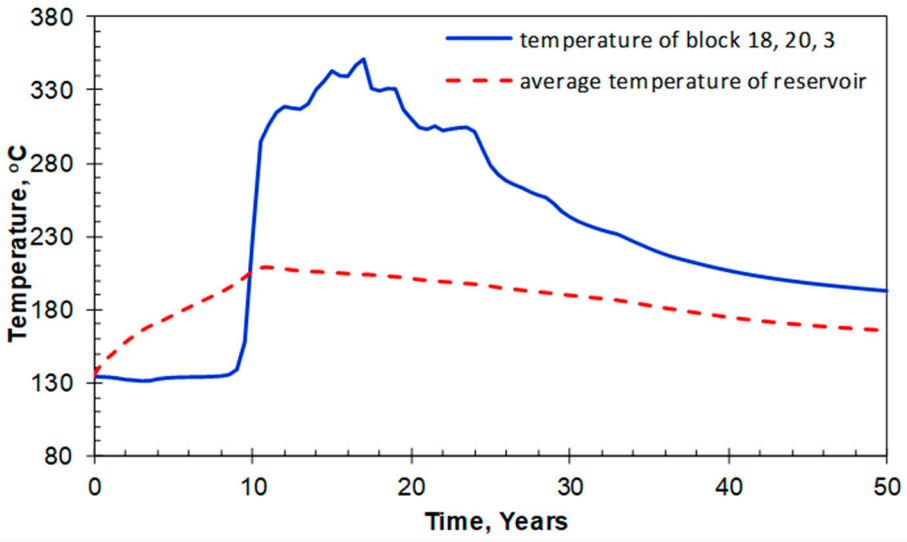

Figure 12. The average reservoir temperature (red dashed line) and the temperature near the heat exchange system wellbore (blue solid line).

As seen in Figure 12, when the combustion front approaches the wellbore (heat exchange system), the temperature around the wellbore increases sharply until reaching a peak point at about 350 °C. With continuous injection of air, the temperature decreases, and this is followed by a long stage of declination. This indicates that a large amount of heat is generated in the reservoir when in situ combustion is applied. Considerable amounts of heat can be extracted by the heat exchanger system from both the surrounding rocks and the combustion reservoir, especially when the peak point of combustion front has been reached.

The coupling between the oil reservoir model and the heat exchanger model is at the depth of the oil reservoir. If the average reservoir temperature is applied (red dashed line in Figure 12) as the boundary condition of the heat exchanger model, this may strongly underestimate the heat production of the heat exchanger. Therefore, in this study, we applied the temperature profile data of the block (18, 20, 3) into the heat exchanger model as a time-dependent boundary condition at the depth of the oil reservoir. This method reduces the computing cost while also preserving the computational validity of the result. This is reasonable, because as can be seen from Figure 10, the affected region in the surrounding rocks is limited to the place very close to the heat exchange wellbore. After applying the temperature data of the block (18, 20, 3) into the proposed heat exchanger model, the outlet temperature was strongly enhanced by the combustion reservoir. The temperature curves are as shown in Figure 13.

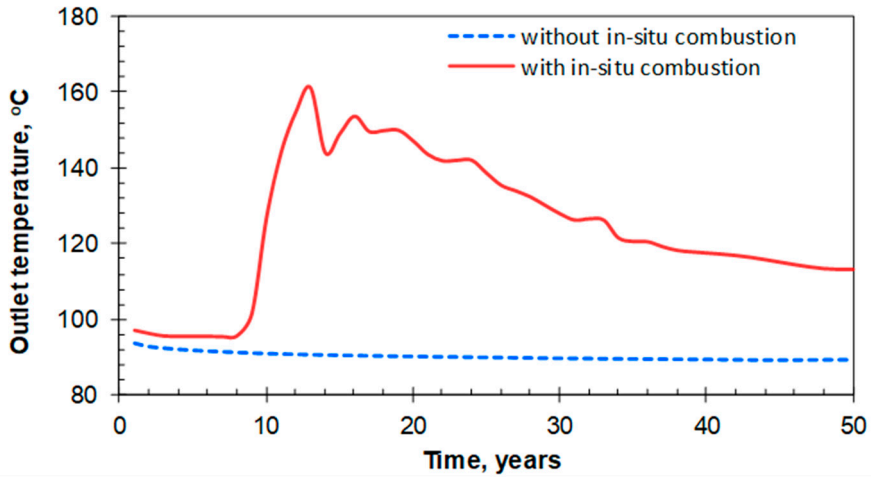

Figure 13. The effect of in situ combustion on performance.

It should be noted that in Figure 13, there is a bump up of the outlet temperature when the combustion front reaches the wellbore. The highest outlet temperature of the extraction well is about 150 °C. An enhancement effect is strongly marked when the geothermal heat is compensated by the in situ combustion technique. The corresponding temperature profiles of the injection annulus and the extraction well are shown in Figure 14.

In Figure 14, the solid lines and dashed lines represent the temperature profiles of the injection annulus and the extraction well, respectively. The lines with different colors show the temperature profiles of the heat exchange system at different operational times. The temperature bump up is also marked in the temperature profiles at the depth of reservoir (4000 m). As seen in Figure 14, before the combustion front reaches the wellbore (in less than 10 years), the temperature of both the injection annulus and the extraction well at the depth of (4000 m) are almost the same, or at least very similar. However, after the combustion front reaches the wellbore (after 10 years), the temperature of the extraction well is significantly higher than that of the injection annulus. This indicates that the in situ combustion has greatly enhanced the temperature of the water in the extraction well.

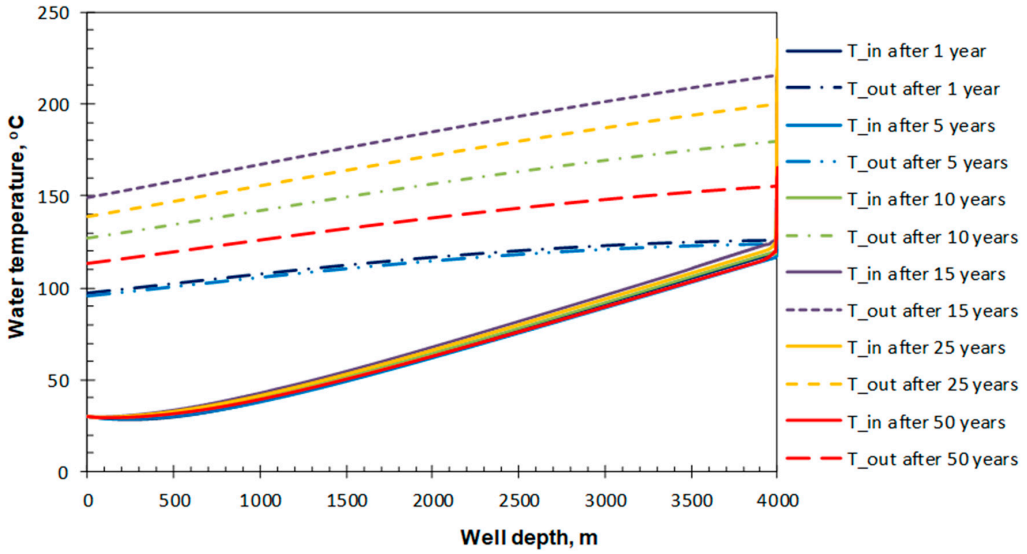

Figure 14. The temperature profiles of different operational time with in situ combustion.

According to Cheng et al. [31], the power provided by the heat exchange system can be simply given by the following equation:

$$P = M(T_{out} - T_{in})C_p\eta_{ri}\eta_m\eta_g/1000 \quad (9)$$

where P is the actual generated power (kW), M is the mass flow rate (kg/s), T_{out} is the outlet temperature of extraction well (K), T_{in} is the inlet temperature of injection annulus (K), C_p is the specific heat capacity of water (J/(kg·K)), η_{ri} is the relative internal efficiency of steam turbine (0.8), η_m is the mechanical efficiency of steam turbine (0.97), η_g is the generator efficiency (0.98) [31]. For this study, the mass flow rate M is calculated by multiplying the injection velocity 0.03 m/s and the cross-sectional area of the injection well (see Figure 6).

Figure 15 demonstrates the variation of the outlet temperature and the actual gained power generated by the heat exchange system as functions of thermal conductivity of the insulation, inlet temperature and the velocity of the injected water in 30 years with in situ combustion.

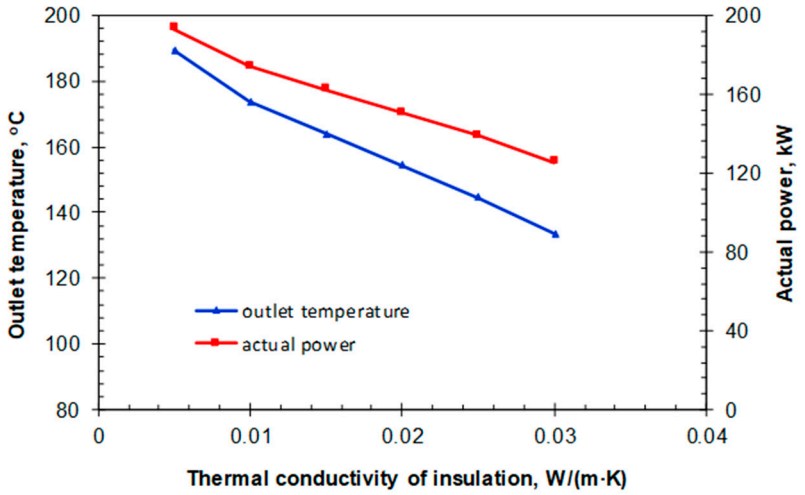

(**a**) Thermal conductivity of the insulation.

Figure 15. *Cont.*

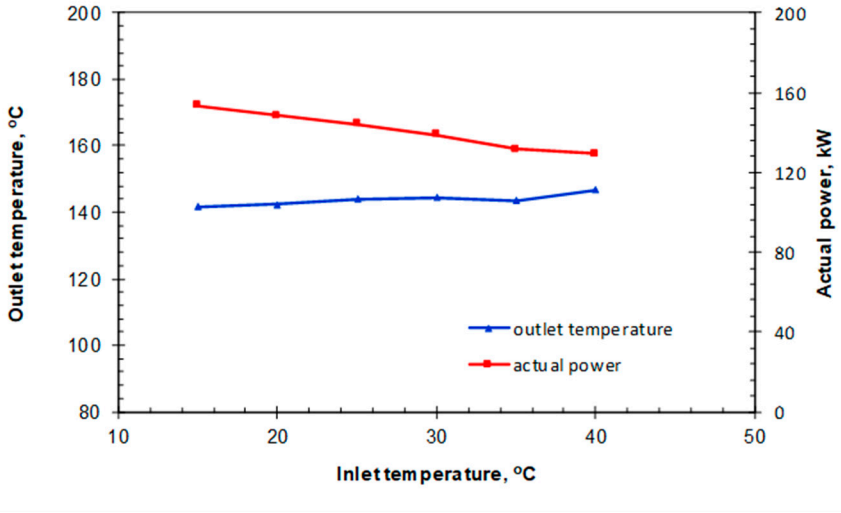

(**b**) Inlet temperature.

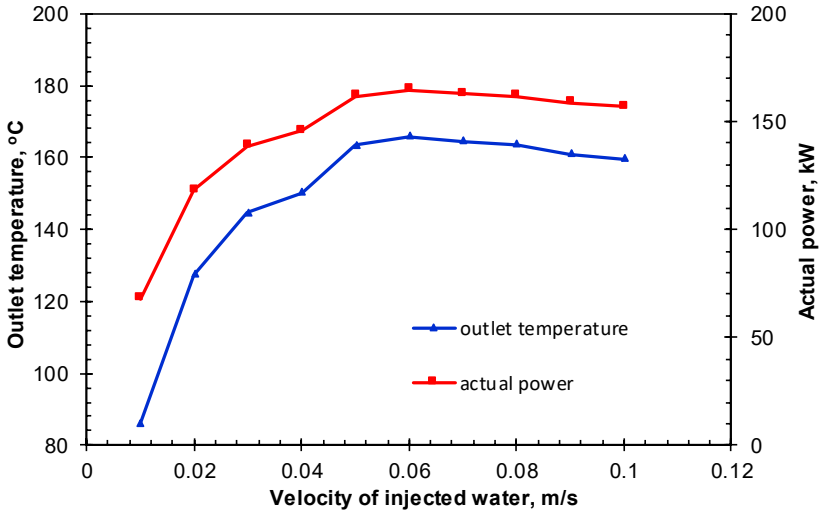

(**c**) Velocity of the injected water.

Figure 15. The variation of the outlet temperature and the actual power of the heat exchange system on different parameters.

It can be seen from Figure 15a,b that when the thermal conductivity of the insulation decreases and the inlet temperature increases, the outlet temperature increases. The outlet temperature is much more sensitive to the value of the thermal conductivity of the insulation. This indicates that insulation with better thermal resistance properties is essential to reducing the heat loss from the extraction well to the injection annulus, and to obtaining higher outlet temperature. This confirms that it helps to extract more heat from the formation. Although there is a higher outlet temperature due to higher inlet temperature, this does not guarantee a higher actual power. The reason for this is that a high inlet temperature does not provide a large temperature difference between the heat exchange system and the surrounding rocks. This reduces the efficiency of the heat transfer from the surrounding rocks to the heat exchange system. In Figure 15c, because of the increase in the velocity of the injected water, both the outlet temperature and the actual power increased first, and then decreased. This is because the water injection velocity has an optimal value of 0.06 m/s. This explains that there is a large amount of heat loss from the extraction well to the injection annulus when the water injection velocity is small.

For situations in which the water injection velocity is larger, the efficiency of the heat extraction from the surrounding rocks to heat exchange system will be very low.

With respect to the temperature near the wellbore of the heat exchange system in the early stage (about 10 years in Figures 13 and 14), it is still not significantly enhanced, even after applying in situ combustion in the reservoir. This means that in situ combustion needs to be applied in advance to avoid the low-temperature stage in order to recover the upfront costs. This is called the advanced in situ combustion method, and comes from a similar concept of advanced water injection technology. In other words, the operation of retrofitting the abandoned well will be executed only when the temperature of the bottom hole increases drastically (i.e., when the combustion front approaches the wellbore).

As can be seen from Figure 16, the outlet temperature of the scenarios without in situ combustion, with in situ combustion, and with advanced in situ combustion are compared. It can be clearly seen that the outlet temperatures of the scenarios without in situ combustion (blue dashed line) and with in situ combustion (red solid line) are relatively low at the beginning. If the heat exchange system starts to operate when the combustion front approaches the area near the wellbore, the outlet temperature will be enhanced significantly at a very early stage, and after that, decrease slowly (green dashed line). To find out how much energy could be extracted by the heat exchange system, the corresponding electricity data were calculated, and are shown in Figure 17.

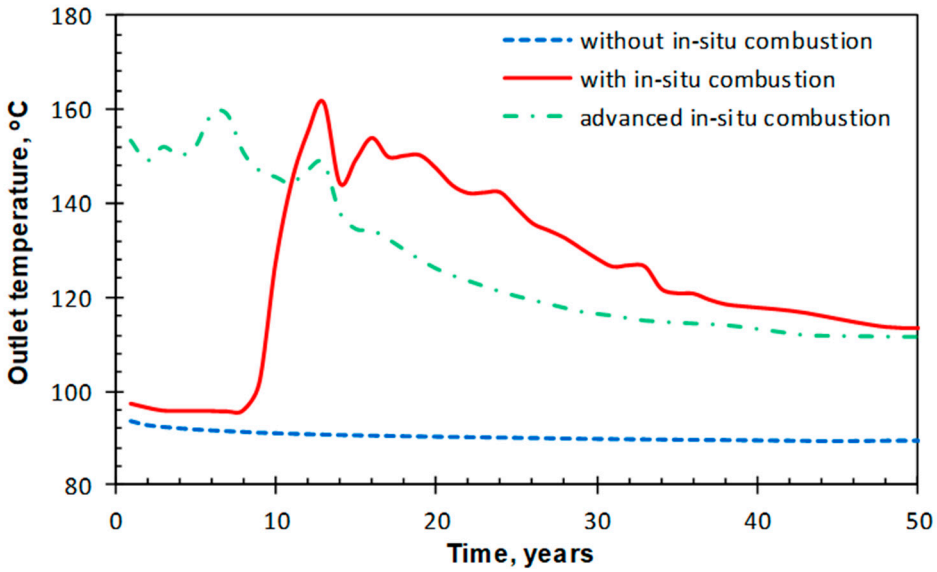

Figure 16. The effect of advanced in situ combustion on performance.

The curves demonstrate that the total electricity generated by the geothermal power plant with compensation for in situ combustion (green dashed line and red solid line) is much more than the electricity generated without in situ combustion (blue dashed line). The cumulative electric energy of the scenario with in situ combustion (red solid line) after a period of 50 years' operation is 50.3×10^6 kW·h. The scenario with advanced in situ combustion (green dashed line) has a higher cumulative electric energy of 51.4×10^6 kW·h.

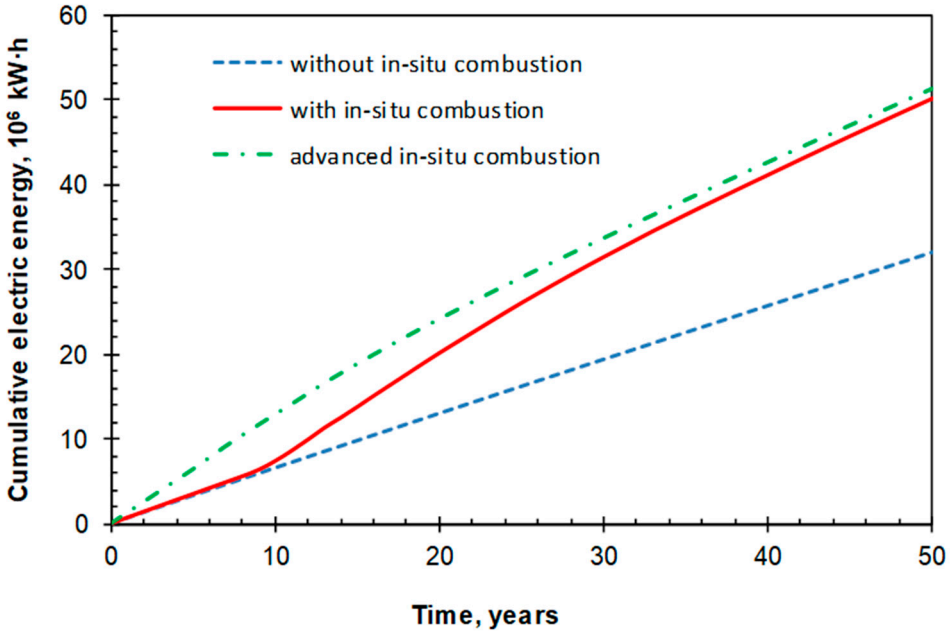

Figure 17. Cumulative electricity generated by the proposed geothermal power system.

4.5. Economic Appraisal

To determine the duration of the payback period of the upfront investment and the cumulative net cash flow after a period of 50 years' operation, an economic appraisal was performed by considering the following information: the geothermal development engineering and management engineering; the requirements of economic appraisal methods and parameters promulgated by China National Development and Reform Commission; the current fiscal and taxation system and the pricing system in China; and the current status of geothermal energy development.

A typical cost for a vertical geothermal well is about $2.3 million, based on the data of the geothermal project in Menengai, Kenya [32]. As stated previously, the cost of work over techniques in such wells is equivalent to about one tenth of the total cost of drilling a new geothermal well [33]. Hence, we assumed that the cost of retrofitting an abandoned well would be $0.23 million for a single well. For the investment of a power plant [34], the cost per installed kW comes to about $1500/kW (power peak is 159.2 kW during the 13th year in these scenarios). Based on the data given by Yambajan geothermal power generation [35], the electricity sale price is $0.14 (¥0.93) per kW·h. The management expense is 1% of the annual sales. The corporate income tax rate is 25%. Therefore, for a period of 50 years in operation, the cumulative net cash flow (NCF) curves are shown in Figure 18.

As shown in Figure 18, the scenario with advanced in situ combustion (green dashed line) has the shortest payback period (about 4.5 years) and the largest final cumulative NCF ($4.94 million). The final cumulative NCF of the two scenarios with in situ combustion (green dashed line and red solid line) are both higher than the scenario without in situ combustion (blue line). Although the scenario with simultaneous in situ combustion (red solid line) has relatively high final cumulative NCF, its payback period is very close to the scenario without in situ combustion (blue dashed line) and it is longer comarable to the scenario with advanced in situ combustion (green dashed line).

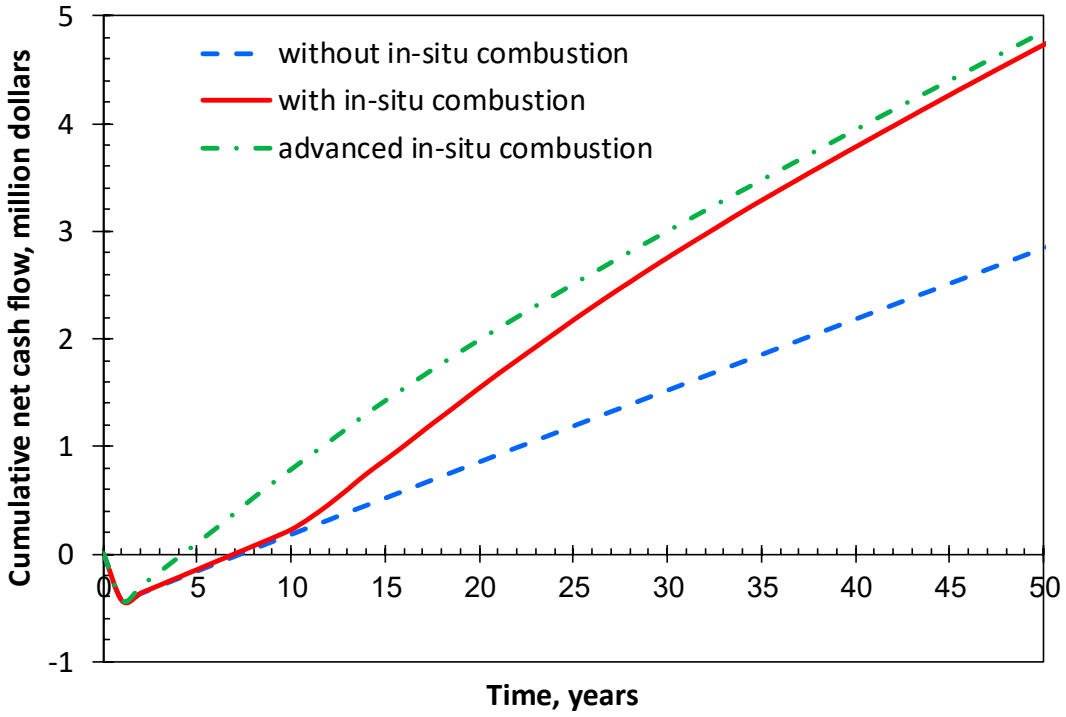

Figure 18. Cumulative net cash flow curves for the proposed geothermal power system.

In regard to the information presented above, a geothermal project with advanced in situ combustion is recommended. Please note that when evaluating geothermal projects, upfront investment, power output, fiscal policy, etc., should be fully considered.

4.6. Discussion

Note that this discussion leads to the conclusions made in this study, and was based upon a correlation of the study model with other previous models. The main theme of this paper is the application of in situ combustion for geothermal development with feasible economic gains. Although Bu et al. [8] and Templeton et al. [29] used different assumptions for their models, their purposes were similar to that of this study: the development of an economically friendly project. What makes the model of this study unique is the introduction of in situ combustion, and the fact that this model considers all of the parameters neglected by the other models. For example, the model of Bu et al. [8] neglects temperature variation in the tube wall of the injection annulus and the extraction well, and further neglects the Dittus-Boelter relation in convection model. The model of Templeton et al. [29] does not consider the rock below the heat exchanger. In short, both studies neglect the changes in the thermal properties of water, which are functions of temperature. Such negligence decreases the accuracy of the temperature distribution and may overestimate the heat extracted from the surrounding rocks in the system. However, since temperature is a major key in geothermal projects, the model proposed in this study considered all these aspects, especially temperature transfer in the extraction well and insulation. The results of this model are fair and reliable, because even with different assumptions from the previous models, the parameters applied are similar. These include the inner diameter of the extraction and the injection wells, the thickness of insulation and casing, the thermal conductivity of the surrounding rocks, the velocity of injected water, geothermal gradient, etc.

Furthermore, during the geothermal fluid extraction process, most models may cause some problems in the formation, such as groundwater recession, corrosion and scaling problems, the high cost of geothermal, and the drilling of the re-injection well, but the newly proposed model has no direct contact with the formation fluid and no effect on oil production; thus, it only extracts the heat from the formation and the oil reservoir by recycling the working fluid in a closed-loop concentric tube, which

is combined with in situ combustion by air injection in the oil reservoir. The coupling between the oil reservoir model and the heat exchanger model is done at the depth of the oil reservoir. This depth may vary for each reservoir, so as not to underestimate the heat production of the heat exchanger. Again, this phenomenon is neglected in the results of the model of Bu et al. [8], and this reduces the accuracy of the simulation results. Note that the experimental data used in this study are similar to those of the two models described above, but the final results, such as temperature, are all different, which is due to the differences in the parameters that are assumed and neglected between the models. However, the results of this study model have more economic benefits than the other two models. A final point to note is that more attention should be paid to the figures, as more detail is apparent in the figures.

5. Conclusions

Based on the calculation and analysis conducted in this study, the following conclusions can be drawn:

(1) An efficient numerical model describing the retrofitting of abandoned wells into geothermal wells with in situ combustion for the purpose of recovering geothermal energy is proposed. The reliability of the model was verified and compared with two other numerical models proposed by Bu et al. [8] and Templeton et al. [29]. The current coupling strategy of the geothermal model is a simple approach for coupling the in situ combustion model and the heat exchanger model.

(2) Several parameters known to affect the system performance were modeled and analyzed using the proposed model in this study. Under specific conditions, the injection velocity has an optimal value of 0.06 m/s. Extreme values (either big or small) of the injection velocity will decrease the efficiency of the heat transfer from the surrounding rocks to the heat exchange system.

(3) The scenarios considered in this study demonstrated that with the help of in situ combustion, the outlet temperature increases remarkably after the combustion front reaches the area near the heat exchange wellbore, which is about 150 °C. The cumulative electricity of the scenarios with in situ combustion and advanced in situ combustion after a period of 50 years of operation are 50.3×10^6 kW·h and 51.4×10^6 kW·h, respectively.

(4) A geothermal system using advanced in situ combustion is proposed to extract more heat from the formation right from the beginning, thereby significantly shortening the payback period of the upfront costs. For this study, the system provides the shortest payback period of 4.5 years and a final cumulative NCF of $4.94 million.

Author Contributions: Conceptualization, C.L. and K.L.; Data curation, C.L.; Formal analysis, Y.Z., C.L. and K.L. Investigation, C.L. Methodology, Y.Z. Software, Y.Z.; Supervision, K.L.; Validation, C.L.; Writing—original draft, Y.Z.; Writing—review & editing, C.L. and K.L.; M.B.M. revised and polished the language of the final version.

Funding: This research received no external funding.

Conflicts of Interest: The authors declare no conflict of interest.

Nomenclature

C_p	specific heat capacity of water, J/(kg·K)
C_p	specific heat capacity of working fluid, J/(kg·K)
G	geothermal gradient, K/m
k	thermal conductivity, W/(m·K)
k_{og}	relative permeability of liquid phase
kr_g	relative permeability of gas phase
kr_{ow}	relative permeability of oil
kr_w	relative permeability of water
M	mass flow rate, kg/s

P	actual generated power, kW
$\vec{q}$	heat flux by conduction, W/m^2
r	radial distance from the central axis, m
R	distance at constant temperature boundary in r direction, m
t	time, s
T	absolute temperature, K
T_{ic}	temperature of reservoir with in situ combustion, K
T_{in}	inlet temperature of injection annulus, K
T_{out}	outlet temperature of extraction well, K
$T_{R,0}$	initial rock temperature, K
$T_{R,b}$	rock temperature at constant temperature boundary, K
T_{srf}	temperature at surface, K
$\vec{u}$	velocity vector, m/s
z	vertical distance from surface, m
Z	distance at constant temperature boundary in z direction, m
η_g	generator efficiency
η_m	mechanical efficiency of steam turbine
η_{ri}	relative internal efficiency of steam turbine,
ρ	density of working fluid, kg/m^3

References

1. Kotler, S. Abandoned Oil and gas Wells Are Leaking. Available online: https://zcomm.org/zmagazine/abandoned-oil-and-gas-wells-are-leaking-by-steven-kotler (accessed on 5 June 2019).
2. Li, T.; Zhu, J.; Xin, S.; Zhang, W. A novel geothermal system combined power generation, gathering heat tracing, heating/domestic hot water and oil recovery in an oilfield. *Geothermics* **2014**, *51*, 388–396. [CrossRef]
3. Zhang, Y.J.; Li, Z.W.; Guo, L.L.; Gao, P.; Jin, X.P.; Xu, T.F. Electricity generation from enhanced geothermal systems by oilfield produced water circulating through reservoir stimulated by staged fracturing technology for horizontal wells: A case study in Xujiaweizi area in Daqing Oilfield, China. *Energy* **2014**, *78*, 788–805. [CrossRef]
4. Lingyu, Z.; Jianguo, Y.; Hongbin, L.; Kewen, L. Energy from Abandoned Oil and Gas Reservoirs. In Proceedings of the SPE Asia Pacific Oil and Gas Conference and Exhibition, Perth, Australia, 20–22 October 2008.
5. Davis, A.P.; Michaelides, E.E. Geothermal power production from abandoned oil wells. *Energy* **2009**, *37*, 866–872. [CrossRef]
6. Wight, N.M.; Bennett, N.S. Geothermal energy from abandoned oil and gas wells using water in combination with a closed wellbore. *Appl. Therm. Eng.* **2015**, *89*, 908–915. [CrossRef]
7. Barbier, E. Geothermal energy technology and current status: An overview. *Renew. Sustain. Energy Rev.* **2002**, *6*, 3–65. [CrossRef]
8. Bu, X.; Ma, W.; Li, H. Geothermal energy production utilizing abandoned oil and gas wells. *Renew. Energy* **2012**, *41*, 80–85. [CrossRef]
9. Nian, Y.L.; Cheng, W.L. Insights into heat transport for thermal oil recovery. *J. Pet. Sci. Eng.* **2017**, *151*, 507–521. [CrossRef]
10. Noorollahi, Y.; Pourarshad, M.; Jalilinasrabady, S.; Yousefi, H. Numerical simulation of power production from abandoned oil wells in Ahwaz oil field in southern Iran. *Geothermics* **2015**, *55*, 16–23. [CrossRef]
11. Mokhtari, H.; Hadiannasab, H.; Mostafavi, M.; Ahmadibeni, A.; Shahriari, B. Determination of optimum geothermal Rankine cycle parameters utilizing coaxial heat exchanger. *Energy* **2016**, *102*, 260–275. [CrossRef]
12. World Energy Council. *World Energy Resources: Geothermal 2016*; World Energy Council: London, UK, 2016.
13. Østergaard, P.A.; Lund, H. A renewable energy system in Frederikshavn using low-temperature geothermal energy for district heating. *Appl. Energy* **2011**, *88*, 479–487. [CrossRef]
14. Self, S.J.; Reddy, B.V.; Rosen, M.A. Geothermal heat pump systems: Status review and comparison with other heating options. *Appl. Energy* **2013**, *101*, 341–348. [CrossRef]

15. Noorollahi, Y.; Mohammadzadeh Bina, S.; Yousefi, H. Simulation of Power Production from Dry Geothermal Well Using Down-hole Heat Exchanger in Sabalan Field, Northwest Iran. *Nat. Resour. Res.* **2016**, *25*, 227–239. [CrossRef]
16. Cinar, M. Creating Enhanced Geothermal Systems in Depleted Oil Reservoirs via In Situ Combustion. In Proceedings of the Thirty-Eighth Workshop on Geothermal Reservoir Engineering, Stanford, CA, USA, 11–13 February 2013.
17. Cheng, W.L.; Liu, J.; Nian, Y.L.; Wang, C.L. Enhancing geothermal power generation from abandoned oil wells with thermal reservoirs. *Energy* **2016**, *109*, 537–545. [CrossRef]
18. Nian, Y.L.; Cheng, W.L. Insights into geothermal utilization of abandoned oil and gas wells. *Renew. Sustain. Energy Rev.* **2018**, *87*, 44–60. [CrossRef]
19. Rabiu Ado, M.; Greaves, M.; Rigby, S.P. Dynamic Simulation of the Toe-to-Heel Air Injection Heavy Oil Recovery Process. *Energy Fuels* **2017**, *31*, 1276–1284. [CrossRef]
20. Hallam, R.J.; Donnelly, J.K. Pressure-up blowdown combustion: A channeled reservoir recovery process. *SPE Adv. Technol. Ser.* **1993**, *1*, 153–158. [CrossRef]
21. Kujawa, T.; Nowak, W.; Stachel, A.A. Utilization of existing deep geological wells for acquisitions of geothermal energy. *Energy* **2006**, *31*, 650–664. [CrossRef]
22. Wang, L.; Li, C.; Liu, S.; Li, H.; Xu, M.; Wang, Q.; Ge, R.; Jia, C.; Wei, G. Geotemperature gradient distribution of Kuqa foreland basin, north of Tarim, China. *Chin. J. Geophys.* **2003**, *46*, 403–407. [CrossRef]
23. Yuan, Y.S.; Ma, Y.S.; Hu, S.B.; Guo, T.L.; Fu, X.Y. Present-day geothermal characteristics in South China. *Chin. J. Geophys.* **2006**, *49*, 1005–1014. [CrossRef]
24. Fu-you, Z. Geothermal Gradient and HeatFlow Characteristics of Nanyang Basin. *Ground Water.* **2016**, *38*, 121–122.
25. Yusong, Y.; Lijun, M.; Gongcheng, Z.; Herong, Z. Some Remarks about Geothermal Gradient of Sedimentary Basins. *Geol. Rev.* **2009**, *55*, 531–535.
26. Liang-Ping, X.; Ju-Ming, Z. Relationship between geothermal gradient and the relief of basement rock in north China plain. *Chin. J. Geophys.* **1988**, *31*, 146–155.
27. Wenquan, T. *Numerical Heat Transfer*; Xi'an Jiaotong University Press: Xi'an, China, 1988.
28. Bird, R.B.; Stewart, W.E.; Lightfoot, E.N. *Transport Phenomena*, 2nd ed.; John Wiley Sons, Inc.: Hoboken, NJ, USA, 2006.
29. Templeton, J.D.; Ghoreishi-Madiseh, S.A.; Hassani, F.; Al-Khawaja, M.J. Abandoned petroleum wells as sustainable sources of geothermal energy. *Energy* **2014**, *70*, 366–373. [CrossRef]
30. Dittus, F.W.; Boelter, L.M.K. Heat transfer in automobile radiators of the tubular type. *Int. Commun. Heat Mass Transf.* **1985**, *12*, 3–22. [CrossRef]
31. Cheng, W.L.; Li, T.T.; Nian, Y.L.; Xie, K. Evaluation of working fluids for geothermal power generation from abandoned oil wells. *Appl. Energy* **2014**, *118*, 238–245. [CrossRef]
32. Kivure, W. *Geothermal Well Drilling Costing—A Case Study of Menengai Geothermal Field*; United Nations University Press: Tokyo, Japan, 2016.
33. Qihua, Z. The Abandoned Well can be Recycled. *China Petrochem.* **2011**, *16*, 26–27.
34. Tocci, L.; Pal, T.; Pesmazoglou, I.; Franchetti, B. Small scale Organic Rankine Cycle (ORC): A techno-economic review. *Energies* **2017**, *10*, 413. [CrossRef]
35. Although Geothermal Generation Enjoys Mature Technology, the Difficulty of Field Application Is Because of Low Feed-in Tariff. Available online: https://www.xianjichina.com/news/details_61970.html (accessed on 21 October 2018).